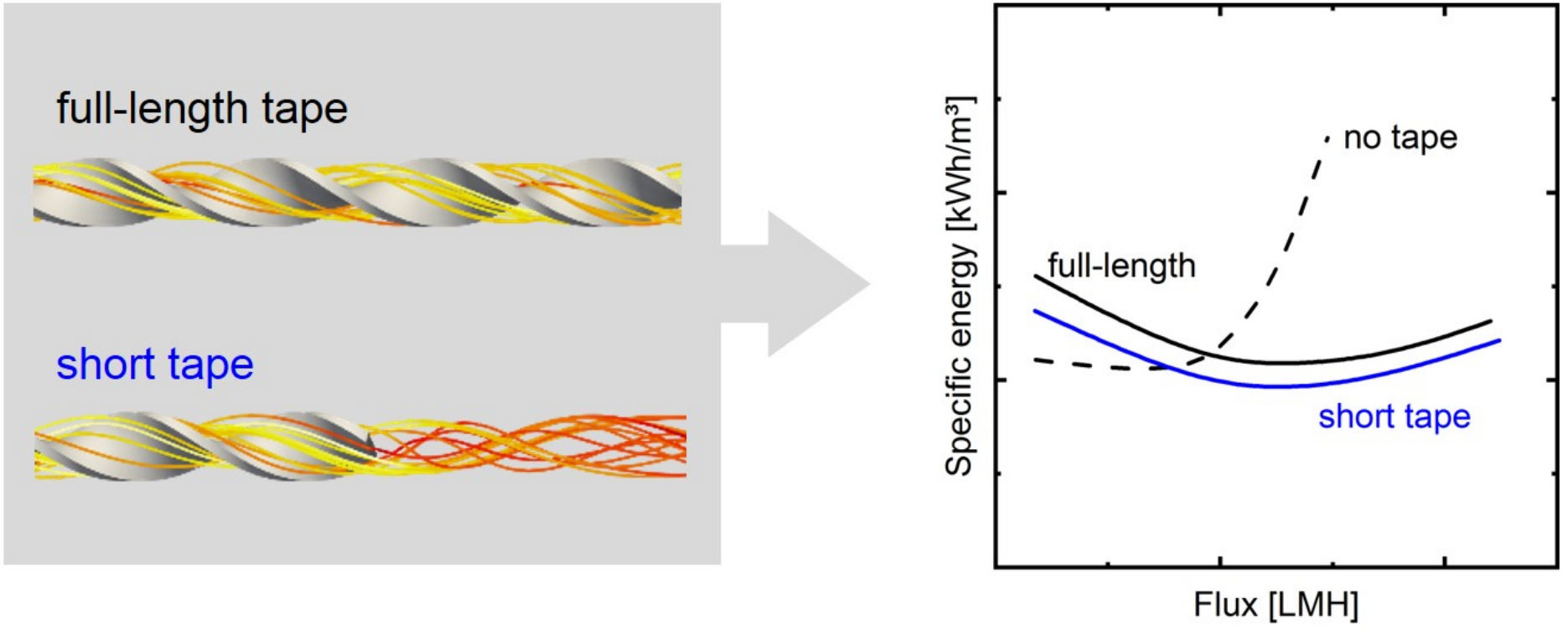
full-length tape
short tape
Specific energy [kWh/m³]
no tape
full-length
short tape
Flux [LMH]

Short and Spaced Twisted Tapes to Mitigate Fouling in Tubular Membranes

Sarah Armbruster[a,*], Felix Stockmeier[a,b,*], Moritz Junker[a], Maira Schiller-Becerra[a], Süleyman Yüce[a], Matthias Wessling[a,b,**]

[a]*RWTH Aachen University, Chemical Process Engineering, Forckenbeckstr. 51, 52074 Aachen, Germany*
[b]*DWI - Leibniz Institute for Interactive Materials, Forckenbeckstr. 50, 52074 Aachen, Germany*

Abstract

Static mixers are an efficient means to mitigate membrane fouling as they deflect the fluid, thus increasing the shear rate at the membrane surface and enhancing back-transport of rejected matter. However, inserting static mixers in the flow channel of a membrane imposes an additional pressure drop. To decrease this detrimental effect of static mixers, we shorten twisted tape mixers and investigate how this shortening translates into a reduction of fouling mitigation. We follow two approaches known from heat transfer enhancement: i) shorten the total length of the twisted tape and ii) use regularly spaced short twisted tape elements which are kept at their position by smooth rods placed in between the twisted elements. Computational fluid dynamics (CFD) is applied to analyze the flow pattern, the shear rate at the membrane and the resulting pressure drop. The results allow for the selection of modified twisted tape mixers with lower pressure loss, but sufficient flow properties for fouling mitigation. The most promising mixer designs were selected according to the CFD study, 3D-printed, and their fouling mitigation effect experimentally investigated using silica suspensions. Additionally, the effect of foulant concentration in this system is analyzed. For low silica concentrations (0.03 g/L) the short and spaced twisted tapes mitigate fouling as efficiently as the full-length twisted tape. At high silica concentrations and fluxes, the full-length mixer mitigates fouling more strongly than the short and spaced twisted tapes. However, the modified twisted tapes prove to be more energy-efficient up to a certain fouling exposure.

Keywords: Turbulence Promoters, Static Mixers, CFD - Computational Fluid Dynamics, Fouling Mitigation, Pressure Drop

1. Introduction

Ultrafiltration processes are often affected by membrane fouling. Fouling can be caused by (a) foulants adsorbed at the membrane surface or in the membrane pores, (b) by foulants forming a gel layer at the membrane surface, and (c) by particles constricting or blocking the pores. Various countermeasures aiming at fouling reduction are applied in industry, and many more have been investigated in research. Mostly, these fouling countermeasures influence the hydrodynamics inside the membrane module, trying to impose fluid instabilities [1] resulting in chaotic and turbulent-like flow conditions. This flow destabilization can either be generated actively, for instance by rotating or vibrating the membrane or the membrane module, or by passive techniques. Passive measures require less additional energy and have no moving parts. Often, they aim at creating secondary flows. Such secondary flows can be introduced by Dean vortices which can evolve in curved channels [2]. Another approach to destabilize the fluid flow is the application of static inserts in a flow channel. These static inserts, also called static mixers or turbulence promoters [3, 4, 5], deflect the fluid in the flow channel. Thus, they induce secondary flows and increase the actual crossflow velocity in the channel as well as the shear rate at the wall. For this reason, inserts have long been used to improve heat transfer in heat exchangers [6, 7, 8, 9]. Static mixers also enhance mixing of the boundary layer. This way concentration polarization is reduced, mass transport amplified and particle back-transport into the bulk promoted. In membrane filtration, static inserts are applied as all these phenomena - fluid deflection, increased shear rate, enhanced mixing

*These authors contributed equally to this work.
**Corresponding Author: M. Wessling
Email address: manuscripts.cvt@avt.rwth-aachen.de (Matthias Wessling)

- help to decrease membrane fouling [3].

2. Background

Research on the application of static mixers in membrane filtration dates back at least to the 1970s [10]. Since then, various geometries and shapes of inserts have been investigated. The simplest geometry is a rod, which is mostly equipped with a wire around its axis to further deflect the fluid [11, 12, 13]. Hence, the number of turns of the wire around the rod can be varied. Either 4 turns per 25 *mm* [11] or per 50 *mm* [13] appears to be the optimal design in terms of flux enhancement when filtering Baker's yeast.

Another quite simple insert is a twisted tape or double helix as it is referred to in some literature [13, 5]. Comparable to the wired rod, the so-called pitch length of the twisted tape can be varied. The pitch length corresponds to the length of one full twist. The pressure drop, as well as the fouling reduction, depend on the pitch length. Decreasing pitch length translates to higher pressure drop, but increased fouling reduction [5, 14].

Modifications of twisted tapes are abundant in literature, especially in the field of heat transfer [15]. Twisted tapes with drilled holes are one example. Such a perforated tape was used, for instance, by Rahimi *et al.* [16] in heat transfer studies. The aim of perforating the tapes is to decrease the pressure drop which they impose on the system [16, 17]. In this case, this is achieved since the fluid can flow through the openings in the insert. Perforated tapes also proved to be beneficial in the microfiltration of milk [17].

Similarly, not only the surface of the inserts can be perforated, but also the edges of the twisted tape can be corrugated, notched or serrated [9, 18, 19, 14]. Notches can be u-shaped, v-shaped, rectangular or circular [9, 20, 21]. Moreover, the cut tape can also be bend such that a wing-like structure evolves [8, 9]. These modifications of twisted tapes have mainly been investigated in heat transfer [8, 9]. In membrane filtration, twisted tapes with a wavy-like edge only had a minor influence on the fouling of humic acid when compared to a standard twisted tape [14].

Twisted tapes usually have a constant diameter along their length. To reduce their pressure drop and the loss of membrane area, static inserts with varying diameters have been investigated. The diameter can decrease linearly with the mixer length and increase sharply in a step [14], or it can increase and decrease regularly, e.g. in a sinusoidal shape [14] or a cone-like structure [22]. An axially varying diameter reduced the pressure loss of the insert. However, tapes with constant diameter caused a higher flux increase than the tapes with varying diameter [14]. When cone-shaped inserts were compared to smooth rods, they reduced fouling to a greater extent than the rods [22].

More complex structures such as Kenics static mixers [4], screw-threaded [23] or blade-type inserts [17] have also been successfully used to improve micro- and ultrafiltration applications. Additive manufacturing, commonly known as 3D printing, enables the fabrication of advanced designs of static inserts. Thus, helically microstructured spacers [24] or spacers based on triply periodic minimal surfaces [25] have been developed for flat sheet applications in ultrafiltration. Furthermore, static inserts for tubular membranes have been fabricated using additive manufacturing [14].

Another approach to decrease the pressure drop associated with the insertion of static mixers is to reduce the length of the mixer. Thus, the volume of the flow channel occupied by the static insert is decreased. Yadav and Padalkar [26] used this approach to enhance the heat transfer of air flow. Applying CFD simulations, they found that the full-length twisted tape gave the highest Nu numbers, but also the highest friction factors for all investigated Re numbers. The half-length twisted tape considerably reduced the friction factor compared to the full-length tape. However, the heat transfer enhancement due to the half-length tape was also lower than that of the full-length tape. Still, the half-length tape showed a $8 - 47$ % higher heat transfer coefficient than the tube without a tape inserted. This was attributed to the preservation of the swirl flow behind the twisted tape. [26]

The approach to use several short twisted tape elements with free space in between as turbulence promoter is based on the same idea as the application of shortened twisted tapes. The swirl flow introduced by a twisted tape is preserved for a certain length behind the twisted tape. Therefore, another twisted tape element is placed behind the first twisted tape, but with some free space in between. Optimally, the free space corresponds precisely to the length within which the swirl flow decays. CFD simulations could deliver data for this optimization to decrease the experimental effort and find optimal solutions. Wang *et al.* [27] optimized the configuration of short-length twisted tapes regarding the heat transfer of turbulent air flow. As optimization parameters, the heat transfer enhancement efficiency and the evolution of the swirl flow were considered. In their case, the optimal free space between two twisted tape elements was 28 - 33 times the inner diameter of the tube which is a very high free space ratio.
The aim of applying spaced twisted tape is again to

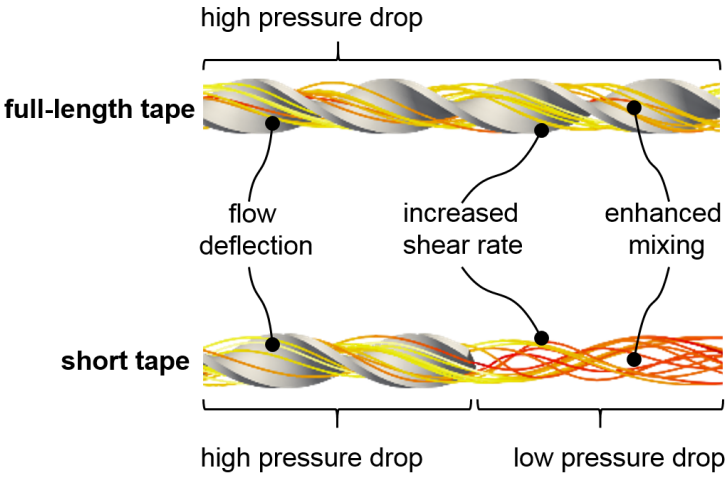

Figure 1: Graphical representation of the approach followed in this study: Using full-length, short and spaced twisted tapes to mitigate membrane fouling. The helical flow pattern remains behind the shorter tape parts. This way the fouling mitigating hydrodynamics continue, but pressure drop is reduced.

reduce the pressure loss induced by the inserts and simultaneously, to maintain the heat or mass transfer enhancement of the full-length twisted tape. Ferroni *et al.* [28] found that regularly spaced twisted tapes decreased the pressure drop by at least 50 % compared to full-length twisted tapes when using liquid water as the medium. Spaced twisted tapes have been successfully tested for improving heat transfer [29, 30, 15, 31]. Eiamsa-ard *et al.* [15], for instance, compared the heat transfer efficiency of full-length and several spaced twisted tapes using a hot and a cold water stream. They found that the full-length tape led to the highest Nu numbers, but also had the highest friction factors. The Nu number and the friction factor of spaced twisted tapes was in between the full-length tape and the empty tube.

As mentioned before, CFD simulation is often used to optimize fluid flow regarding pressure loss [32, 33, 34]. Flow simulations also have the advantage of supplying additional information that is otherwise hard to measure in experiments, e.g. shear stress [35, 36, 37, 38]. Another advantage of flow simulations is the possibility to investigate complex insert structures which might be complicated to fabricate. Jung and co-workers [39] analyzed numerically the fouling mitigation of barrier-embedded partitioned pipe mixers in cross-flow filtration using the concentration boundary layer thickness and the wall concentration as parameters to measure the effectiveness of the inserts.

To the best of our knowledge, neither short nor spaced twisted tapes have been investigated in the field of mass transfer. The combined experimental and simulation study presented below analyzes how short and spaced twisted tapes affect membrane fouling in comparison to a full-length twisted tape. CFD simulations are performed where twisted tapes with various lengths and different free space ratios are investigated to reduce the experimental effort. The different tapes are compared regarding shear rate, flow pattern and pressure drop. The most promising short and spaced twisted tapes are fabricated via 3D printing and experimentally investigated using silica colloids as model foulants. Furthermore, the silica concentration is varied to study its influence on membrane fouling and the fouling mitigation by the static mixers. Fig. 1 shows a graphical representation of the approach followed in this study.

3. Materials and Methods

3.1. Chemicals and membrane

Colloidal silica (Ludox HS40, Sigma Aldrich) was used as model foulant. Concentrations of 0.03 g/L, 0.12 g/L, 0.24 g/L and 0.60 g/L colloidal silica in a 20 mM phosphate buffer at pH 8 were applied in the fouling experiments. The tubular ceramic ultrafiltration membrane (atech innovations GmbH, Germany) had a nominal cut-off of 100 kDa, an inner diameter of 6 mm and a length of 0.25 m. One of the membranes had an active filtration area of 0.0043 m^2 and a pure water permeability of 450 LMH/bar, the second membrane of the same type had an active area of 0.0041 m^2

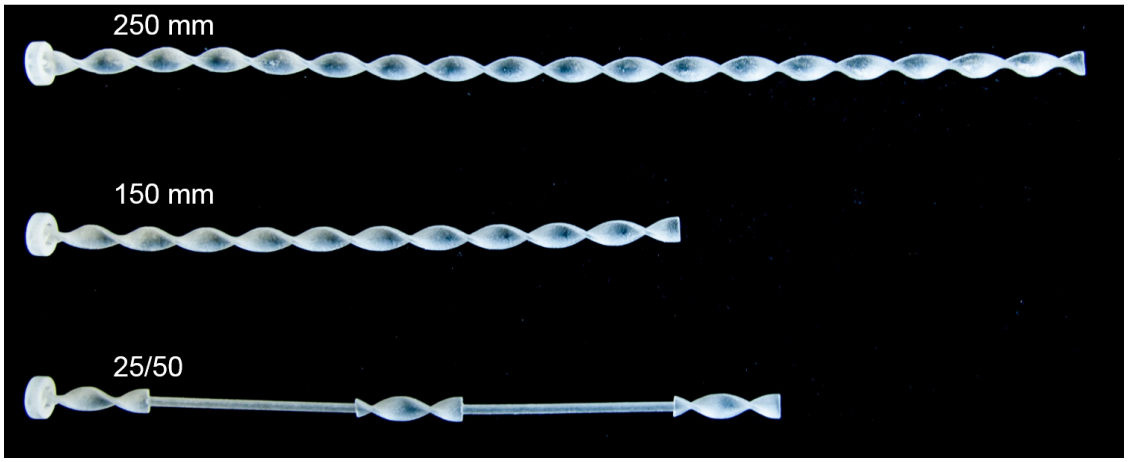

Figure 2: Photo of three experimentally investigated static mixers. Above, the full-length twisted tape, in the middle a short twisted tape and beneath a spaced twisted tape having twisted tapes with a length of 25 *mm* and 50 *mm* long rods in between.

and pure water permeability of around 650 LMH/bar. In between fouling experiments, the membranes were cleaned by flushing the filtration system with 10 L of hot water (temperature around 50 $^{\circ}C$) at a flow rate of 60 L/h and a subsequent flushing step using deionized water at the same flow rate. During cleaning, the retentate was not recycled.

3.2. Static mixers

All static mixer geometries are based on a twisted tape shape. The diameter of all mixers was 5.5 *mm* and their thickness 1 *mm*. The pitch length, which corresponds to the length of one twisted element, was 13.75 *mm*. Two types of twisted tapes were investigated. The first type represents twisted tapes of different length ranging from 100 *mm* to 250 *mm* in 50 *mm* steps. The second type were so-called spaced twisted tapes. They consist of multiple shorter twisted tapes connected by smooth rods that had a diameter of 2 *mm*. The primary function of the rods is to connect the mixer sequences and keep them at defined positions. However, they also have a small influence on the flow profile, shear rates and consequently fouling reduction. They decrease the area of the flow channel and impose a doughnut-shape on the flow. The following three designs of the spaced twisted tapes were used:

- combination 50/50: alternating 50 *mm* twisted tape and 50 *mm* smooth rod
- combination 25/25: alternating 25 *mm* twisted tape and 25 *mm* smooth rod
- combination 25/50: alternating 25 *mm* twisted tape and 50 *mm* smooth rod (see Fig. 2)

Fig. 2 exemplary shows three static mixer geometries which were experimentally investigated. The full-length twisted tape is the uppermost tape with a length of 250 *mm*, beneath, a short twisted tape and one type of spaced twisted tape are displayed.

In total, seven twisted tape geometries, a smooth rod (diameter: 2 *mm*, length: 250 *mm*), and the empty flow channel of the tubular membrane were investigated using CFD. Based on the CFD results, five of the seven static mixer geometries were selected for fabrication and experimentally investigated. These were the twisted tape with full length (250 *mm*, corresponding to the length of the membrane), a twisted tape with a length of 200 *mm* and one with a length of 150 *mm*. In addition, two of the spaced twisted tapes were fabricated: combination 25/25 and combination 25/50. The mixers were manufactured in-house by polyjet 3D printing (Stratasys, Objet Eden 260V, resolution: 32 μm) and consist of a photosensitive acrylate-based polymer (Stratasys, RGD810). A second polymer (Stratasys, SUP705) is printed to support the mixers during the printing process. Subsequently, this support structure was removed in a bath of 1 M NaOH solution.

3.3. Filtration Set-Up

All filtration experiments (pure water permeability, fouling, cleaning) were carried out using a Titan Osmo Inspector (Convergence Industry B.V., The Netherlands). A simplified flow sheet of the system is shown in Fig. 3. The pressures of feed, retentate, and permeate can be measured. In the feed and permeate, two Coriolis mass flow controllers measure and control the flow rates by controlling the diaphragm pump and the pres-

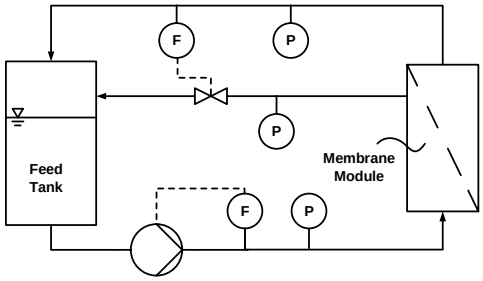

Figure 3: Flow sheet of the experimental set-up. Permeate and retentate were collected in the feed tank and fully recycled.

sure retention valve in the retentate line, respectively. The system allows for constant flux filtration monitoring a feed-side pressure increase as indicator for concentration polarization and fouling.

3.4. Computational Fluid Dynamics

For the design of shortened mixers that exhibit a similar flow pattern and fouling mitigation at reduced pressure loss, detailed knowledge of the hydrodynamics inside the membrane is needed. The developing flow pattern, resulting shear rates and the pressure loss were therefore evaluated using the CFD software COMSOL Multiphysics.

For simulation, the inner membrane diameter was assumed to match the diameter of the twisted tapes (5.5 *mm*) to improve mesh construction and convergence properties. Additionally, an inflow section of 10 *mm* was added for laminar flow profile development. For modeling fluid flow along a membrane, it is reasonable to neglect the transport through the membrane, as the permeate flux is small compared to feed flow [40]. Hence, it is widely acknowledged in the literature to assume the membrane as impermeable for simulation [41]. In the system used in this work, the ratio of permeate to feed flow was 4.7 % at maximum allowing for the same assumption. Silica particles were neglected as well since they do not influence the fluid properties at low concentrations, as was shown in rheology experiments.

The Reynolds number is $Re \approx 2060$ for pure water properties at 30 $^{\circ}C$, atmospheric pressure, a tube diameter of 5.5 *mm* and an inlet velocity of 0.3 m/s. Hence, a stationary laminar flow model with incompressible flow was applied.

For single phase incompressible laminar flow, COMSOL solves the Navier-Stokes equations. These equations describe the conservation of momentum (Eq. 1) and mass (Eq. 2).

Table 1: Measured viscosity η of deionized water and silica suspensions with the indicated concentrations at 30$^{\circ}C$. Given are the viscosity values averaged for shear rates from 10 s^{-1} to 100 s^{-1}. The standard error SE of triplicate measurements is stated in addition.

	DI	silica concentration		
	water	0.12 g/L	0.24 g/L	0.60 g/L
η [mPa · s]	0.761	0.772	0.836	0.838
SE [mPa · s]	0.017	0.024	0.057	0.082

$$\rho\left(\frac{\delta\vec{v}}{\delta t} + \vec{v}\cdot\nabla\vec{v}\right) = -\nabla p + \eta\nabla\vec{v} + \vec{F} \quad (1)$$

$$\nabla\cdot\vec{v} = 0 \quad (2)$$

Here ρ is the density, $\vec{v}$ the velocity, p the pressure, η the dynamic viscosity and $\vec{F}$ is the sum of external forces applied to the fluid. The finite element method with linear shape functions was used in COMSOL for discretization.

The meshing was successively refined by increasing the degrees of freedom until a stable result was obtained. The pressure drop along the module was used as a control parameter. A number of mesh elements above $3\cdot10^5$ was found to be sufficient, see supplementary material.

3.5. Viscosity Measurements

The viscosity of the silica suspensions was measured in a double gap system at 30$^{\circ}C$ using a Discovery Hybrid Rheometer HR3 (TA Instruments, USA). 12 *mL* sample of each solution was measured at shear rates ranging from 1 s^{-1} to 4000 s^{-1}. The viscosity of DI water was measured in comparison.

The viscosity was found to be constant in a wide range of shear rates, and similar to water for all suspensions. Hence, an average value for the viscosity of each fluid was calculated from the measured values at shear rates from 10 s^{-1} to 100 s^{-1}. The mean viscosities are given in Tab. 1 and used to calculate the filtration resistance (Eq. 3).

3.6. Fouling Experiments

Colloidal silica (Ludox HS40) was used as a model foulant. The fouling was assessed using the improved flux step method by van der Marel *et al.* [42]. In this method, the flux is increased stepwise to a maximum flux and decreased to the initial flux. In between the high flux steps, a flux relaxation step is applied. Thus, the reversibility of fouling by flux relaxation can be assessed. During the experiments, the transmembrane pressure (TMP) is measured, and the feed flow rate kept

constant at 30 L/h. The high flux levels were applied for 10 *min* and the flux relaxation steps for 5 *min*. For the highest silica concentrations of 0.24 g/L and 0.60 g/L, transmembrane pressures of up to 20 *bar* were reached. High flux steps were aborted as soon as a TMP of 17 *bar* was reached to keep the stability limits of set-up and tubing. An exemplary fouling experiment for a system without a static mixer and one with a static mixer (twisted tape with 150 *mm* length) is shown in Fig. 4. The influence of the static mixer is already clearly visible as the TMP levels remain constant over almost all flux levels as compared to the TMP increase for the experiments without static mixer.

The total filtration resistance R was calculated according to Eq. 3. Here, the transmembrane pressure TMP is divided by the viscosity η and the permeate flux J. The measured viscosity averaged in the range of 10 s^{-1} to 100 s^{-1}, was used in the calculations. For the silica suspension with a concentration of 0.03 g/L, the measured viscosity of pure water was applied.

$$R = \frac{TMP}{\eta \cdot J} \tag{3}$$

Furthermore, the energy dissipated during the filtration process was considered. The dissipated energy E_{diss} consists of two parts; the energy dissipated due to cross-flow and the energy dissipated due to filtration. Eq. 5 shows the resulting calculation as given by Fane and Chang [43]. The energy dissipated due to cross-flow was calculated by multiplying the pressure drop along the membrane with the feed flow rate (first term in Eq. 5). Theoretically, an average flow rate at the feed side should be used instead of the feed flow rate. As, however, the stage-cut in the experiments never exceeded 4.7 %, this difference was neglected and the feed flow rate used. Additionally, the hydraulic energy dissipated by filtration was considered as the second contribution to the total dissipated energy. The energy dissipated by filtration was obtained by multiplying TMP with permeate flow rate (second term of Eq. 5).

$$E_{diss} = \Delta p \cdot Q_F + TMP \cdot Q_P \tag{4}$$

$$= (p_F - p_R) \cdot Q_F + \frac{p_F + p_R}{2} \cdot Q_P \tag{5}$$

Q denotes the volumetric flow rate, TMP the transmembrane pressure and p the pressure. The subscript F refers to feed, R to retentate and P to permeate.

The dissipated hydraulic energy describes the energy which is lost as it is converted into friction losses, mixing and heat. Hence, it can also be considered as the energy that reduces fouling. Static mixers obstruct the flow, induce eddies and vortices. Therefore, they increase the pressure drop along the membrane. As this pressure drop substantially contributes to the hydraulic dissipated energy, the additional energy required due to the insertion of static mixers is already included in E_{diss}.

By relating the dissipated energy to the obtained amount of permeate, the specific dissipated energy E_{sp} in kWh per m^3 permeate was received (Eq. 6). E_{diss} is divided by the permeate flow rate Q_P or by flux J times filtration area A.

$$E_{sp} = \frac{E_{diss}}{Q_P} = \frac{\Delta p \cdot Q_F}{J \cdot A} + TMP \tag{6}$$

TMP, filtration resistance and specific dissipated energy during the flux step experiments were analyzed to compare the fouling mitigation capabilities of the different mixers. All experiments were carried out in triplicates, and the standard error is indicated as error bars.

4. Results and Discussion

4.1. Computational Fluid Dynamic Simulations

CFD simulations were conducted for seven different mixers, the empty tube and a tube with a centered smooth rod. The generated data was an indication for the selection of five static mixers for experiments. Here, the parameters for filtration performance analyzed are conservation of flow pattern, shear rate enhancement and pressure loss.

Twisted tape static mixers enforce a helical flow pattern in a tubular membrane lumen. This flow pattern already proved effective for fouling reduction [5, 14]. Therefore, the development and preservation of this pattern is a key aspect when estimating the effectiveness of different twisted tape configurations. The magnitude of the velocity perpendicular to the membrane axis acts as a quantitative measure for the preservation of the helical flow pattern. Fig. 5a shows the flow pattern for three representative twisted tapes, a full-length tape, a shorter 150 *mm* tape and a spaced tape with 25 *mm* tape and 50 *mm* connector.

The flow pattern and rotational velocity in a tube with inserted 250 *mm* twisted tape were used as a reference in the analysis. If a twisted tape does not cover the whole tube, the helical flow pattern exponentially decreases behind the twisted tape parts. For example, behind a 150 *mm* twisted tape it is still sufficiently strong for a distance of around 50 *mm*. The transition to laminar tubular flow is after a distance of about 100 *mm*. There is a direct correlation between flow pattern and velocity

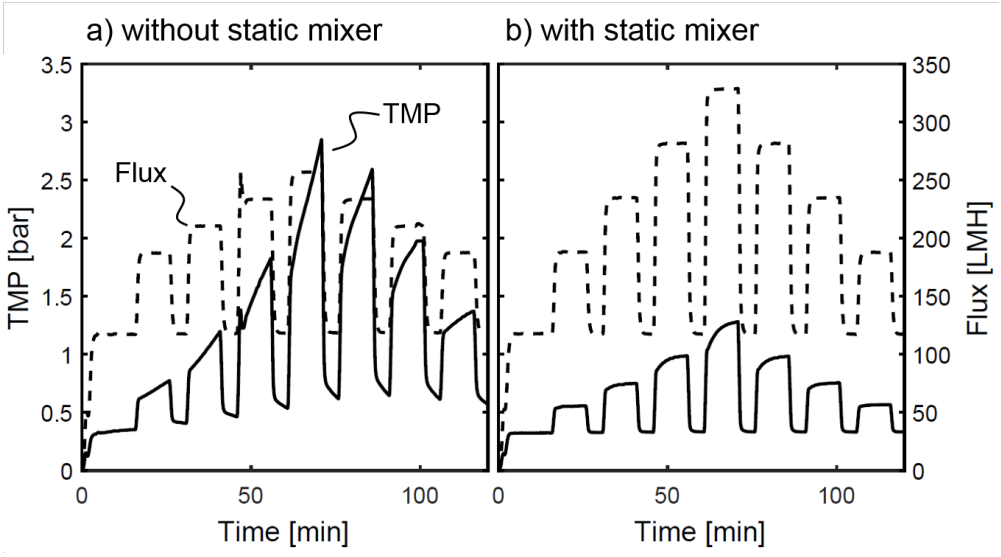

Figure 4: Flux step method. In a), a fouling experiment for the conventional filtration system without a static mixer is displayed (silica concentration: 0.03 g/L). In b), the same flux steps are applied for a system with a static mixer. Exemplary, an experiment is shown where a twisted tape with a length of 150 *mm* was applied, and 0.03 g/L silica were used.

perpendicular to the membrane surface. The decrease of the velocity perpendicular to the surface velocity behind a 25 *mm* twisted tape and a 150 *mm* twisted tape is compared in Fig. 6. The flow pattern develops in the same way for both mixers. The distance until the velocity declines to 30 % of its maximum value is used for the development of a spaced static mixer. Based on this result, a combination of 25 *mm* twisted tape parts connected by 50 *mm* smooth rods with 2 *mm* diameter is chosen. With this design, the flow pattern is preserved over the whole membrane length, see Fig. 5a.

The average wall shear rate is a major quantity for evaluating the anti-fouling potential of a static mixer [43]. It represents forces that lift particles off the membrane surface. A comparison of the simulated average shear rates potentially deduces the mixers effectiveness. Fig. 5b shows the average wall shear rate for a full length twisted tape, a shorter 150 *mm* tape and a spaced tape with 25 *mm* tape and 50 *mm* connector. The minimum value corresponds to the shear rate of 719 s^{-1} at the wall of an empty membrane lumen. The average shear rate is 2543 s^{-1} when inserting a full-length twisted tape. For the rest of the twisted tapes, only the shear rate at membrane wall sections without tape is considered. Behind a 150 *mm* tape, the averaged shear rate decreases to 1190 s^{-1}. The spaced approach exhibits higher shear rates between twisted tape parts. In this case, the average shear rate is 1683 s^{-1}. The sections behind twisted tapes show the preservation of the helical flow pattern similar to Fig. 5a.

Five twisted tapes were selected for further experiments based on the previous results. The shortened 200 *mm* mixer is promising, because the helical flow pattern and, thus, the wall shear rate is maintained until the end of the membrane. However, increased shear rates over the whole module can also be seen in the simulation of the 150 *mm* twisted tape. The tape and rod combination all introduce high shear rates at decreased pressure losses. The 25/50 combination is chosen, because it has the lowest pressure loss, and the 25/25 combination generates the highest average wall shear rates. The full length 250 *mm* mixer is used as a reference.

4.2. Pressure Drop

Pressure drop is an important quantity for filtration performance since it correlates directly with the dissipated hydraulic energy. The application of twisted tapes increases the axial pressure drop over the length of the membrane. To determine the pressure drop of the static mixers, the pressure loss of the empty tube was subtracted from the total pressure loss of the systems with a mixer (see Eq. 8). Inlet and outlet pressure were measured at the same positions as feed and retentate pressure during filtration.

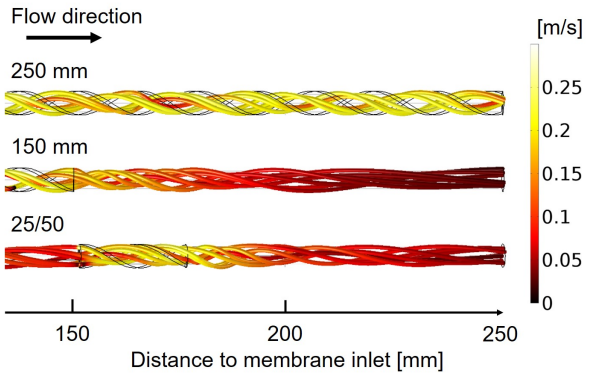

(a) Flow pattern

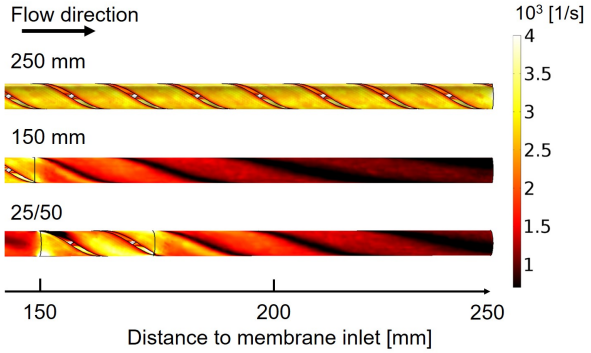

(b) Shear rate

Figure 5: Simulated flow pattern and shear rate for the full length tape (250 *mm*), the shorter tape with a length of 150 *mm* and the spaced tape with 25 *mm* tape and 50 *mm* connector. The helical flow and the shear are preserved for around 50 *mm* after the mixers' end. The last 100 *mm* of the tubular membrane are displayed. Darker colors represent lower rotational velocities or shear rates, lighter colors higher velocities and shear rates.

$$\Delta p_{mixer} = \Delta p_{total,mixer} - \Delta p_{empty} \quad (7)$$

$$= (p_{in} - p_{out})_{total,mixer} - (p_{in} - p_{out})_{empty} \quad (8)$$

The pressure loss over the length of the module was used to validate the CFD simulations. To have similar conditions for simulations and experiments, the pressure loss for the different twisted tapes was measured with pure water under no permeation (closed permeate outlet). In Fig. 7, simulated and measured pressure losses of different static mixers are compared. Assuming ideal conditions in the CFD approaches lead to a distinguishable difference between simulation and experiment. For example, the tubing before and behind the module, the surface roughness of the membrane, and the influence of the silica are not taken into account in

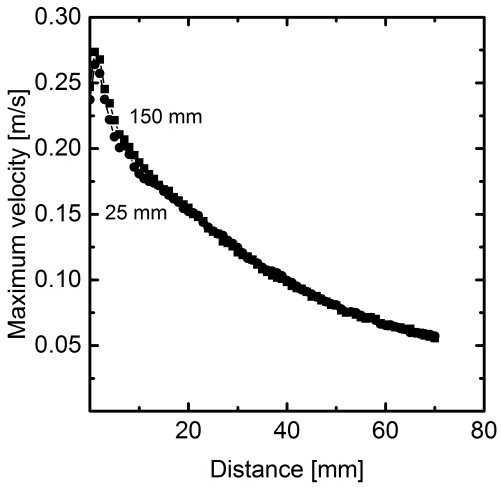

Figure 6: Maximum value of velocity component perpendicular to the flow direction depending on the distance to the twisted tape element. Overlapping simulation results for a 150 *mm* twisted tape and a 25 *mm* long twisted tape.

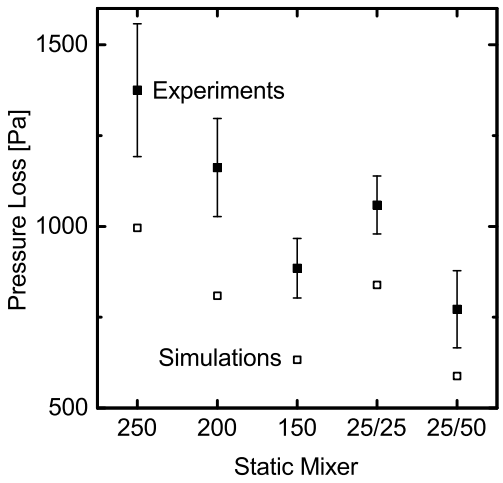

Figure 7: Pressure loss of the different static mixers as obtained numerically (CFD simulation, open symbols) and experimentally (closed symbols). The numbers on the x-axis denote the length of the twisted tapes, and for the spaced twisted tapes, the numbers indicate the length of the twisted elements/length of free space. The pressure loss was measured with pure water and without permeation in the experiments. Error bars are standard error of triplicate measurements.

the CFD simulations. However, both the measured and the simulated pressure drop data show the same trend and are in agreement regarding the order of magnitude (see Fig. 7).

As expected, the shorter the twisted tape, the smaller is the additional pressure drop of the insert (see Fig. 7). This trend is visible for both the measured and the simulated pressure drop. Additionally, the 25/25-combination of spaced twisted tapes shows a higher pressure loss than the 25/50-combination, again both for the experimental and simulation results. The different pressure loss of the two spaced twisted tapes can be explained by the difference in 'free' space in between the twisted elements, the different number of twisted elements and the different total length of the combinations. The 25/25-combination consists of five twisted tape elements (each 25 *mm* long) and four 'free space' elements in the form of a smooth rod (2 *mm* in diameter, 25 *mm* long). In contrast, the 25/50-combination has only three twisted tape elements (also each 25 *mm* long) and two smooth rods (50 *mm* long) keeping the twisted elements apart. Hence, the 25/50-combination shows a smaller total length and less twisted elements as well as a smaller total twisted length compared to the 25/25-combination. These differences in shape explain the lower pressure drop of the 25/50-combination.

4.3. Filtration Resistance

Fouling experiments were performed with different silica concentrations (0.03 g/L to 0.60 g/L) and several twisted tapes as well as a standard filtration system without any fouling mitigation measure. In Fig. 8, the total resistance is shown for the applied flux steps. For the lowest silica concentration of 0.03 g/L, the filtration resistance of the membrane without static mixer increased rapidly from the beginning. This increase became even stronger for fluxes exceeding 200 LMH. At the highest analyzed flux of 248 LMH, the filtration resistance reached $5.27 \cdot 10^{12}\ m^{-1}$ which is almost five times the intrinsic membrane resistance. If a static mixer is applied during filtration, the resistance is substantially lower and reached less than $2 \cdot 10^{12}\ m^{-1}$ for the highest investigated flux of around 320 LMH. Hence, fouling was significantly reduced compared to the system without a mixer. From Fig. 8a, it can be concluded that the differences within the full-length, short and spaced twisted tapes which have been investigated, are negligible for a silica concentration of 0.03 g/L.

The silica concentration was step-wise increased to further investigate the differences in fouling mitigation capabilities of the different twisted tapes. When using a four times higher concentration of 0.12 g/L silica, the resistance of the full-length twisted tape was the lowest of the analyzed twisted tapes for all fluxes. The difference between full-length tape and twisted tape modifications became significant at fluxes above 235 LMH as Fig. 8b shows. For the highest flux of 328 LMH, the resistance of the 150 *mm* long twisted tape was lower than the resistance of the system with spaced twisted tape. This result indicates that the short twisted tape induces a higher wall shear rate and a flow pattern which is better suited to mitigate fouling. The three 25 *mm* long elements of the spaced twisted tape led to a lower increase in wall shear rate. Therefore, the increase in silica concentration from 0.03 g/L to 0.12 g/L already led to distinct differences in the fouling mitigation of the different twisted tapes.

The same trend continued for higher silica concentrations. At 0.24 g/L, the filtration resistance of the system with inserted 250 *mm* twisted tape significantly increased to $16.13 \cdot 10^{12} 1/m$ at 326 LMH, see Fig. 8c. Under these conditions, the 150 *mm* and spaced twisted tape mitigated fouling to the same extent, reaching a filtration resistance of about $19 \cdot 10^{12} 1/m$. The difference in performance seen at 0.12 g/L silica concentration did not get larger with increasing concentration.

At the highest silica concentration of 0.60 g/L, fouling became even more severe in all systems, see Fig. 8. The filtration resistance at low fluxes is comparable for all twisted tapes and also comparable to the experiments with lower silica concentration. As soon as fluxes over 200 LMH were applied, the filtration resistance rose exponentially for all investigated systems, see Fig. 8d. For the short and the spaced twisted tape, flux steps above 236 LMH had to be aborted due to the overshooting TMP, rapidly reaching more than 17 *bar*. For the system with full-length twisted tape, it was possible to apply a higher flux of 281 LMH. However, Fig. 8d clearly shows that the resistance was with $21 \cdot 10^{12}\ m^{-1}$ extremely high. Different from the lower silica concentrations, the system with full-length twisted tape showed an exponential increase in filtration resistance at 0.60 g/L silica. Still, inserting a full-length twisted tape can increase the range of operating conditions up to 242 LMH in the tested system.

All in all, the full-length twisted tape reduced fouling to the greatest extent for all investigated fluxes and silica concentrations. The short twisted tape with a length of 150 *mm* and the spaced twisted tape (combination 25/50) showed similar behavior but led to higher filtration resistances than the full-length twisted tape. At the lowest silica concentration of 0.03 g/L, however, the modified twisted tape reduced fouling as well as the full-length twisted tape. Therefore, it could be

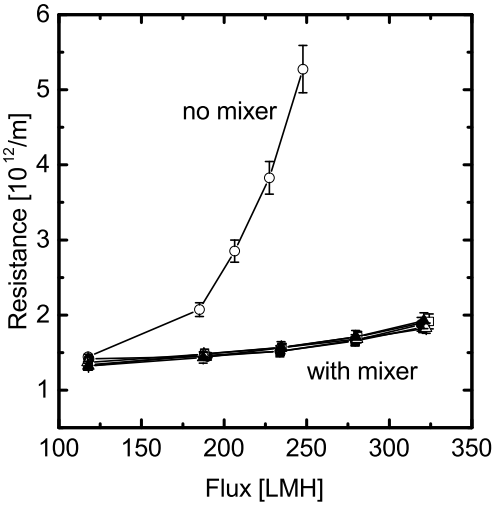

(a) 0.03 g/L silica

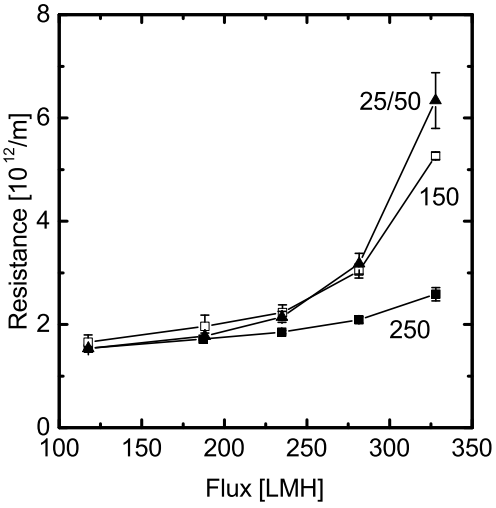

(b) 0.12 g/L silica

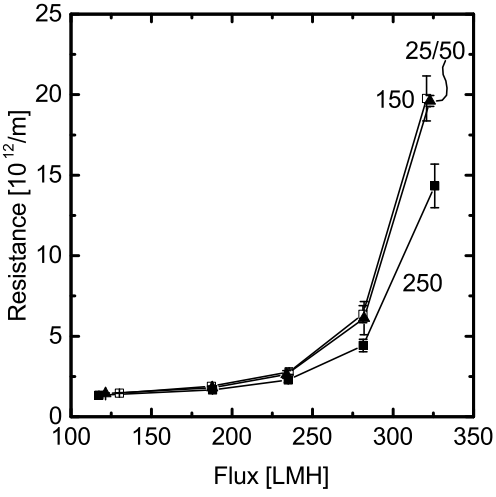

(c) 0.24 g/L silica

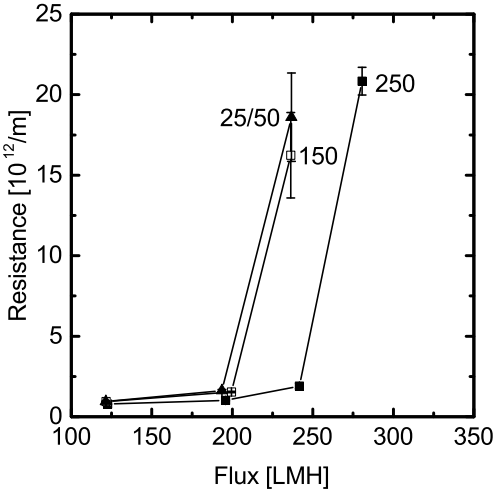

(d) 0.60 g/L silica

Figure 8: Filtration resistance vs flux for all systems with mixer and four different silica concentrations. Error bars are standard error of triplicate measurements. Note the different y-scales.

proven that shortening the twisted tape and using spaced twisted tapes can be sufficient in terms of fouling reduction. Additionally, it was shown that it depends on the filtration conditions if the shear rate enhancement and swirl flow induced by the modified twisted tapes suffice or not to keep the filtration resistance at a viable level. To further assess the process efficiency of static inserts, their influence on energy demand for filtration needs to be quantified.

4.4. Specific Dissipated Energy

To analyze the energy efficiency of the twisted tape inserts, the specific dissipated energy was determined. It relates the energy dissipated by pumping and filtration to the obtained amount of permeate, see Eq. 5 and Eq. 6. Figs. 9 and 10 show the specific energy vs. flux for all experiments. When considering the lowest silica concentration of 0.03 g/L, the empty membrane with no turbulence promoter showed the lowest specific energy consumption at a flux of 185 LMH, Fig. 9. However, the specific energy increases exponentially with increasing flux. As fouling increases with rising flux, the filtration resistance increases as well and the TMP has to be raised to maintain the desired flux. Therefore also the specific dissipated energy increases.

Fig. 9 shows that all energy curves posses a minimum. The minima result from competing effects contributing to the specific energy. On the one hand, the pressure drop along the membrane decreases slightly with increasing flux since the average crossflow velocity is reduced by the higher stage-cut. Additionally, the pressure drop is divided by the permeate flow rate to obtain the specific dissipated energy due to crossflow. Hence, the specific dissipated energy for pumping decreases at higher fluxes. This effect is even more prominent if a twisted tape is inserted, because of a higher pressure loss.
On the other hand, the specific energy consumption increases with higer transmembrane pressure needed to obtain higher fluxes. This influence gets more prominent with rising flux.
Altogether, these effects lead to a minimum in energy consumption for all systems with twisted tapes. The minimum is not as visible for the system without twisted tape since the necessary low fluxes were not measured in this study. However, Fig. 9 clearly shows that up to a flux of around 235 LMH, the filtration in the systems with a mixer is dominated by pressure drop, whereas, for higher fluxes, the effect of TMP is dominating. In conclusion, the application of static mixers is particularly interesting in the TMP-dominated region. Additionally, the insertion of twisted tapes shifts the optimum operating conditions, defined as the minimum specific energy consumption, to higher fluxes. The higher specific dissipated energy of the system with a 25/25-spaced twisted tape in comparison to the full-length tape, in Fig. 9b, indicates that the introduced wall shear rate is too low for efficient fouling prevention.

Experiments with higher silica concentration were only possible by use of twisted tapes due to severe fouling. Fig. 10 shows the specific energy consumption for 0.12 g/L, 0.24 g/L and 0.60 g/L silica concentration. At 0.12 g/L, see Fig. 10a, the full-length twisted tape introduces the highest specific energy consumption in the pressure drop dominated regime. When reaching the TMP-dominated regime, the modified twisted tapes exhibit a faster increase in specific energy consumption breaking even with the full-length tape at a flux of 280 LMH. Hence, it depends on the flux region and the extent of fouling if the application of a full-length twisted tape or a short or spaced twisted tape is more energy-efficient.

For 0.24 g/L and 0.60 g/L silica, all types of analyzed twisted tapes start with the same specific energy consumption for the lowest flux step as Fig. 10b and Fig. 10c show. The specific energy consumption of the full-length twisted tape always stays equal or below the modified versions. For 0.60 g/L silica, high flux experiments needed to be skipped due to overshooting TMP. Only the full-length twisted tape allowed for a higher flux. These experiments reinforce the assumption of a TMP-dominated regime where better fouling mitigation results in lower specific energy consumption. The optimum operating condition also shifts to higher fluxes depending on the fouling potential.

5. Conclusion

The present study investigated the effect of short and spaced twisted tapes on fouling mitigation in tubular ceramic membranes. CFD simulations of the flow field, shear rate and pressure drop for different short and spaced twisted tapes were performed to reduce the experimental effort and gain additional data. The length of the short tapes, as well as the length of the twisted parts and the free space in case of the spaced twisted tapes, were varied. Comparing the simulated with experimentally measured pressure drop along the flow channel, the simulation model could be successfully validated. In the simulations, the short tape with a length of 150 *mm* (instead of 250 *mm*) and the spaced twisted tapes with 25 *mm* twisted tape and 25 *mm* or 50 *mm* free space gave similar flow pattern and shear rates as the full-length twisted tape. Therefore, these modifications of twisted

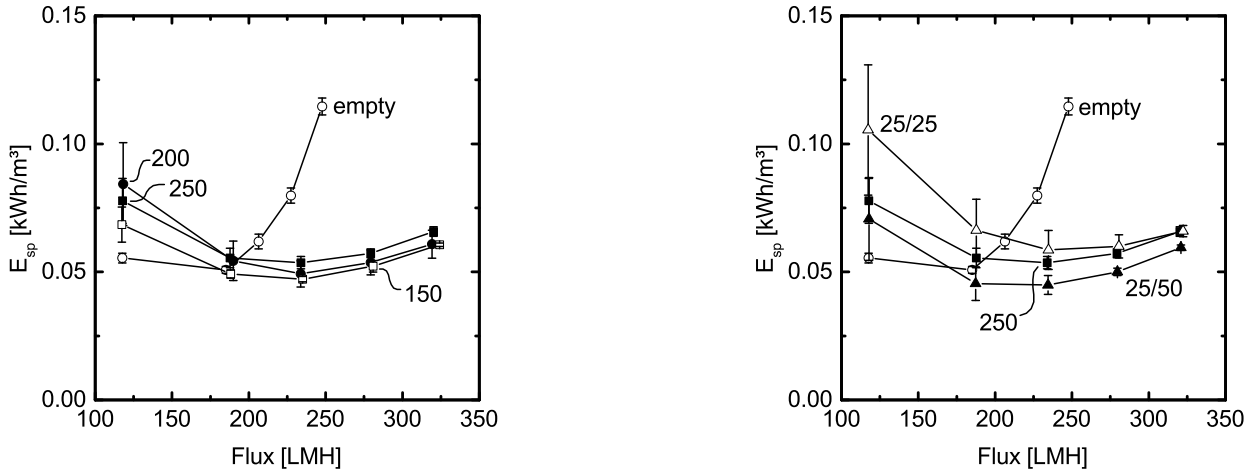

(a) short twisted tapes

(b) spaced twisted tapes

Figure 9: Specific dissipated energy vs flux for the system without mixer and all systems with mixer at a silica concentration of 0.03 g/L. The specific energy of the system without tape and the one with full-length twisted tape are shown for comparison. Error bars display standard error of triplicate measurements.

tapes were fabricated via 3D printing and intensively investigated in fouling experiments. Four concentrations of colloidal silica suspensions were used. At the lowest investigated concentration of 0.03 g/L, all modified twisted tapes mitigate fouling as well as the full-length twisted tape. As the pressure drop induced by the modified tapes turned out to be considerably lower than that of the full-length tape, the specific dissipated energy of all modified tapes was reduced in the low flux range in comparison to the full-length twisted tape. Compared to the membrane without turbulence promoter, the systems with mixers showed a decreased specific energy consumption for fluxes above 200 LMH.

At higher silica concentrations, the full-length twisted tape led to markedly reduced filtration resistances in comparison to the modified twisted tapes. The difference was more pronounced the higher the applied flux and the higher the silica concentration. In terms of specific dissipated energy, however, the modified twisted tapes profit from lower pressure losses. Thus, the modified tapes have a lower energy consumption in the pressure drop-dominated regime. The full-length twisted tape develops an advantage with increasing fouling potential. In the TMP-dominated regime, high wall shear rates over the whole membrane length are most effective.

In conclusion the application of twisted tapes is not only possible and proven in heat transfer, but is also suitable for enhanced mass transfer and improved fouling prevention in membrane processes. A pressure drop- and a TMP-dominated regime were also defined with a recommendation of effective twisted tape designs. Reducing the membrane area covered by the twisted tape by using modified twisted tapes proved to have a positive effect on specific dissipated energy in the pressure drop-dominated regime. In the TMP-dominated regime, a full-length twisted tape performed best because of its stronger fouling reduction. Therefore, the aim of reducing the pressure drop of turbulence promoters without losing performance was reached with restriction to the pressure drop-dominated regime.

Acknowledgement

The authors acknowledge financial support from the ERA-NET Susfood-CEREAL project, No. 031A431B, by the German Federal Ministry of Education and Research. This project has also received funding from the European Research Council (ERC) under the European Unions Horizon 2020 research and innovation program (grant agreement no. 694946).

References

[1] H. B. Winzeler, G. Belfort, Enhanced performance for pressure-driven membrane processes: the argument for fluid instabilities, Journal of Membrane Science 80 (1) (1993) 35–47.

[2] T. Luelf, C. Bremer, M. Wessling, Rope coiling spinning of curled and meandering hollow-fiber membranes, Journal of Membrane Science 506 (2016) 86–94.

[3] S. Popović, M. Wessling, Turbulence promoters in membrane processes, Journal of Membrane Science, Virtual Special Issue.

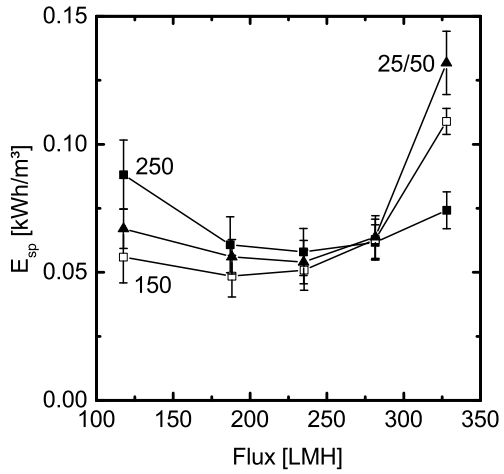

(a) 0.12 g/L silica

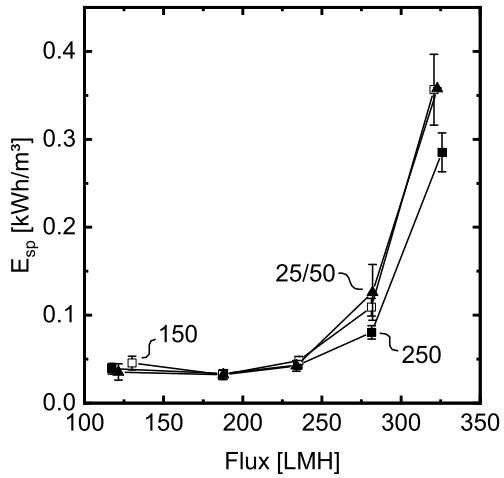

(b) 0.24 g/L silica

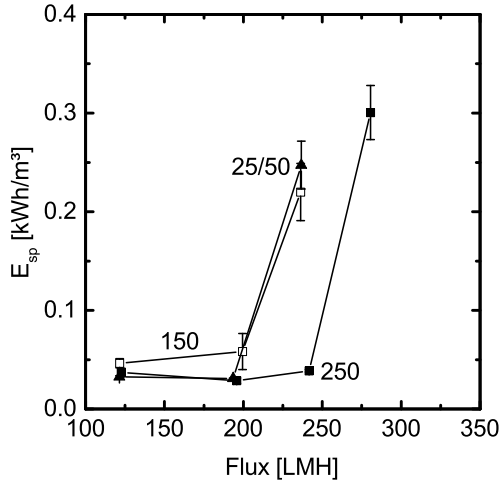

(c) 0.60 g/L silica

Figure 10: Specific dissipated energy vs flux for the systems with mixer and three different silica concentrations. Error bars display standard error of triplicate measurements.

[4] D. M. Krstic, M. N. Tekic, M. D. Caric, S. D. Milanovic, Kenics static mixer as turbulence promoter in cross-flow microfiltration of skim milk, Separation Science and Technology 38 (7) (2003) 1549–1560.

[5] S. Popović, M. N. Tekić, Twisted tapes as turbulence promoters in the microfiltration of milk, Journal of Membrane Science 384 (12) (2011) 97–106.

[6] S. Yce, Wrmebergang an viskoelastische Flssigkeiten in statischen Mischern, Ph.D. thesis, Aachen, aachen, Techn. Hochsch., Diss., 1990 (1990).
URL `http://publications.rwth-aachen.de/record/73869`

[7] R. M. Manglik, A. E. Bergles, Heat transfer and pressure drop correlations for twisted-tape inserts in isothermal tubes: Part II - Transition and turbulent flows, Journal of Heat Transfer 115 (4) (1993) 890–896.

[8] S. W. Chang, M. H. Guo, Thermal performances of enhanced smooth and spiky twisted tapes for laminar and turbulent tubular flows, International Journal of Heat and Mass Transfer 55 (25) (2012) 7651–7667.

[9] A. Hasanpour, M. Farhadi, K. Sedighi, A review study on twisted tape inserts on turbulent flow heat exchangers: The overall enhancement ratio criteria, International Communications in Heat and Mass Transfer 55 (2014) 53–62.

[10] E. W. Pitera, S. Middleman, Convection promotion in tubular desalination membranes, Industrial & Engineering Chemistry Process Design and Development 12 (1) (1973) 52–56.

[11] B. Gupta, J. Howell, D. Wu, R. Field, A helical baffle for cross-flow microfiltration, Journal of Membrane Science 102 (1995) 31–42.

[12] H. Yeh, K. Chen, Improvement of ultrafiltration performance in tubular membranes using a twisted wire-rod assembly, Journal of Membrane Science 178 (1) (2000) 43–53.

[13] A. L. Ahmad, A. Mariadas, K. K. Lau, Flux enhancement by introducing turbulence effect for microfiltration of saccharomyces cerevisiae, Separation Science and Technology 40 (6) (2005) 1213–1225.

[14] S. Armbruster, O. Cheong, J. Lölsberg, S. Popovic, S. Yüce, M. Wessling, Fouling mitigation in tubular membranes by 3D-printed turbulence promoters, Journal of Membrane Science 554 (2018) 156–163.

[15] S. Eiamsa-ard, C. Thianpong, P. Promvonge, Experimental investigation of heat transfer and flow friction in a circular tube fitted with regularly spaced twisted tape elements, International Communications in Heat and Mass Transfer 33 (10) (2006) 1225–1233.

[16] M. Rahimi, S. R. Shabanian, A. A. Alsairafi, Experimental and CFD studies on heat transfer and friction factor characteristics of a tube equipped with modified twisted tape inserts, Chemical Engineering and Processing: Process Intensification 48 (3) (2009) 762–770.

[17] S. Popović, D. Jovičević, M. Muhadinović, S. Milanović, M. Tekić, Intensification of microfiltration using a blade-type turbulence promoter, Journal of Membrane Science 425 (2013) 113–120.

[18] S. W. Chang, Y. J. Jan, J. S. Liou, Turbulent heat transfer and pressure drop in tube fitted with serrated twisted tape, International Journal of Thermal Sciences 46 (5) (2007) 506–518.

[19] P. Seemawute, S. Eiamsa-ard, Thermohydraulics of turbulent flow through a round tube by a peripherally-cut twisted tape with an alternate axis, International Communications in Heat and Mass Transfer 37 (6) (2010) 652–659.

[20] B. Salam, S. Biswas, S. Saha, M. M. K. Bhuiya, Heat transfer enhancement in a tube using rectangular-cut twisted tape insert, Procedia Engineering 56 (2013) 96–103.

[21] A. Hasanpour, M. Farhadi, K. Sedighi, Experimental heat trans-

fer and pressure drop study on typical, perforated, v-cut and u-cut twisted tapes in a helically corrugated heat exchanger, International Communications in Heat and Mass Transfer 71 (Supplement C) (2016) 126–136.

[22] V. Mavrov, N. Nikolov, M. Islam, J. Nikolova, An investigation on the configuration of inserts in tubular ultrafiltration module to control concentration polarization, Journal of Membrane Science 75 (1) (1992) 197–201.

[23] S. Najarian, B. Bellhouse, Enhanced microfiltration of bovine blood using a tubular membrane with a screw-threaded insert and oscillatory flow, Journal of Membrane Science 112 (2) (1996) 249–261.

[24] C. Fritzmann, M. Wiese, T. Melin, M. Wessling, Helically microstructured spacers improve mass transfer and fractionation selectivity in ultrafiltration, Journal of Membrane Science 463 (2014) 41–48.

[25] N. Sreedhar, N. Thomas, O. Al-Ketan, R. Rowshan, H. H. Hernandez, R. K. Abu Al-Rub, H. A. Arafat, Mass transfer analysis of ultrafiltration using spacers based on triply periodic minimal surfaces: Effects of spacer design, directionality and voidage, Journal of Membrane Science 561 (2018) 89–98. doi:10.1016/j.memsci.2018.05.028.

[26] R. Yadav, A. Padalkar, CFD analysis for heat transfer enhancement inside a circular tube with half-length upstream and half-length downstream twisted tape, Journal of Thermodynamics 2012.

[27] Y. Wang, M. Hou, X. Deng, L. Li, C. Huang, H. Huang, G. Zhang, C. Chen, W. Huang, Configuration optimization of regularly spaced short-length twisted tape in a circular tube to enhance turbulent heat transfer using CFD modeling, Applied Thermal Engineering 31 (6) (2011) 1141–1149.

[28] P. Ferroni, R. E. Block, N. E. Todreas, A. E. Bergles, Experimental evaluation of pressure drop in round tubes provided with physically separated, multiple, short-length twisted tapes, Experimental Thermal and Fluid Science 35 (7) (2011) 1357–1369.

[29] S. Saha, U. Gaitonde, A. Date, Heat transfer and pressure drop characteristics of laminar flow in a circular tube fitted with regularly spaced twisted-tape elements, Experimental Thermal and Fluid Science 2 (3) (1989) 310–322.

[30] A. W. Date, U. N. Gaitonde, Development of correlations for predicting characteristics of laminar flow in a tube fitted with regularly spaced twisted-tape elements, Experimental Thermal and Fluid Science 3 (4) (1990) 373–382.

[31] P. Eiamsa-ard, N. Piriyarungroj, C. Thianpong, S. Eiamsa-ard, A case study on thermal performance assessment of a heat exchanger tube equipped with regularly-spaced twisted tapes as swirl generators, Case Studies in Thermal Engineering 3 (2014) 86–102.

[32] O. Kavianipour, G. D. Ingram, H. B. Vuthaluru, Investigation into the effectiveness of feed spacer configurations for reverse osmosis membrane modules using Computational Fluid Dynamics, Journal of Membrane Science 526 (2017) 156–171. doi:10.1016/j.memsci.2016.12.034.

[33] W. Zhang, X. Ruan, Y. Ma, X. Jiang, W. Zheng, Y. Liu, G. He, Modeling and simulation of mitigating membrane fouling under a baffle-filled turbulent flow with permeate boundary, Separation and Purification Technology 179 (2017) 13–24. doi:10.1016/j.seppur.2017.01.022.

[34] S. Al-Sharif, M. Albeirutty, A. Cipollina, G. Micale, Modelling flow and heat transfer in spacer-filled membrane distillation channels using open source CFD code, Desalination 311 (2013) 103–112. doi:10.1016/j.desal.2012.11.005.

[35] A. Saeed, R. Vuthaluru, Y. Yang, H. B. Vuthaluru, Effect of feed spacer arrangement on flow dynamics through spacer filled membranes, Desalination 285 (2012) 163–169. doi:10.1016/j.desal.2011.09.050.

[36] G. Guillen, E. M. Hoek, Modeling the impacts of feed spacer geometry on reverse osmosis and nanofiltration processes, Chemical Engineering Journal 149 (1-3) (2009) 221–231. doi:10.1016/j.cej.2008.10.030.

[37] M. Shakaib, S. Hasani, M. Mahmood, CFD modeling for flow and mass transfer in spacer-obstructed membrane feed channels, Journal of Membrane Science 326 (2) (2009) 270–284. doi:10.1016/j.memsci.2008.09.052.

[38] D. Wypysek, D. Rall, M. Wiese, T. Neef, G.-H. Koops, M. Wessling, Shell and lumen side flow and pressure communication during permeation and filtration in a multibore polymer membrane module, Journal of Membrane Science accepted for publication.

[39] S. Jung, H. Jung, T. G. Kang, K. Ahn, Fouling mitigation in crossflow filtration using chaotic advection: a numerical study, AIChE JournalSubmitted to AIChE Journal.

[40] I. Gaspar, P. Tekic, A. Koris, A. Krisztina, S. Popovic, G. Vatai, CFD and laboratory analysis of axial cross-flow velocity in porous tube packed with differently structured static turbulence promoters, Hemijska industrija 69 (6) (2015) 713–718. doi:10.2298/HEMIND140312001G.

[41] S. Ahmed, M. Taif Seraji, J. Jahedi, M. A. Hashib, CFD simulation of turbulence promoters in a tubular membrane channel, Desalination 276 (1-3) (2011) 191–198. doi:10.1016/j.desal.2011.03.045.

[42] P. van der Marel, A. Zwijnenburg, A. Kemperman, M. Wessling, H. Temmink, W. van der Meer, An improved flux-step method to determine the critical flux and the critical flux for irreversibility in a membrane bioreactor, Journal of Membrane Science 332 (12) (2009) 24–29.

[43] A. Fane, S. Chang, Techniques to enhance performance of membrane processes, in: A. Pabby, S. Rizvi, A. Requena (Eds.), Handbook of Membrane Separations: Chemical, Pharmaceutical, Food, and Biotechnological Applications, Taylor & Francis, Boca Raton, FL, USA, 2008, pp. 193–232.